Journal of Sound and Vibration 331 (2012) 5408–5423

Contents lists available at SciVerse ScienceDirect

Journal of Sound and Vibration

journal homepage: www.elsevier.com/locate/jsvi

Sound transmission loss of metamaterial-based thin plates with multiple subwavelength arrays of attached resonators

Yong Xiao [a,b], Jihong Wen [a,b], Xisen Wen [a,b,*]

[a] Vibration and Acoustics Research Group, Laboratory of Science and Technology on Integrated Logistics Support, National University of Defense Technology, Changsha 410073, China
[b] MOE Key Laboratory of Photonic and Phononic Crystals, National University of Defense Technology, Changsha 410073, China

ARTICLE INFO

Article history:
Received 18 January 2012
Received in revised form
17 June 2012
Accepted 11 July 2012
Handling Editor: I Lopez Arteaga
Available online 4 August 2012

ABSTRACT

This paper is concerned with sound transmission loss of metamaterial-based thin plates consisting of multiple subwavelength arrays of spring–mass resonators attached to an unbounded homogenous thin plate. Two analytical wave approaches are developed for the calculation of diffuse field sound transmission loss of such metamaterial-based thin plates. Numerical results show that a metamaterial-based plate can result in much higher sound transmission loss than a bare plate (with the same surface mass density) at frequencies within the mass-law region and the coincidence region. It is also demonstrated that by using an extremely thin plate to form a metanaterial-based plate, the construction can be implemented as a potential sound insulation material with good performance at low frequencies.

1. Introduction

Metamaterials are generally considered to be artificial composites containing subwavelength microstructures that exhibit unusual properties not readily available in nature. This concept was first developed in the field of electromagnetic wave propagation [1,2], but recently, the acoustic analogs have attracted increasing attention [3–5]. Acoustic metamaterials comprising subwavelength arrays of resonant units have been shown to exhibit negative mass density [3,6,7], negative modulus [5], and double negative characteristics [4]. The development of acoustic metamaterials provides some new ideas for the manipulation of wave motion in acoustic media, such as the design of acoustic cloaks and low-frequency sound insulation materials [3].

One type of acoustic metamaterial that has received much interest is known as the locally resonant sonic material [3], consisting of subwavelength arrays of coated spheres (the coating is elastically soft material while the sphere is high density solid) immersed in a matrix medium. The locally resonant sonic material can realize sonic band gaps at low frequencies with a periodicity order(s) of magnitude smaller than the relevant sonic wavelength. Experimental investigations of such locally resonant sonic materials have demonstrated significant attenuation of sound waves in the low audible frequency region [3,8,9]. The idea of locally resonant sonic material has also been extended to the design of locally resonant engineering structures, such as rods [10,11], beams [12,13] and plates [14–18], for the purpose of suppressing elastic wave propagation in these structures. More recently, lightweight membrane-type acoustic

* Corresponding author at: Vibration and Acoustics Research Group, Laboratory of Science and Technology on Integrated Logistics Support, National University of Defense Technology, Changsha 410073, China.
Tel./fax: +86 731 8457 4975.
E-mail addresses: xiaoyong.nudt@gmail.com (Y. Xiao), wenxs@vip.sina.com (X. Wen).

0022-460X/$ - see front matter © 2012 Elsevier Ltd. All rights reserved.
http://dx.doi.org/10.1016/j.jsv.2012.07.016

metamaterials have been developed to achieve high sound transmission loss (STL) over a broad low-frequency range (50–1000 Hz) [19–21]. Such acoustic metamaterials are fabricated by using an elastic membrane fixed on a rigid frame with a small mass attached to the center of each framed cell. The sound insulation mechanism of such constructions is explained by a near-total reflection achieved at a frequency between two eigenmodes where the average normal displacement of the membrane is zero [19,20,22].

While the idea of introducing arrays of local resonators into a host medium to form acoustic metamaterials was proposed about 10 years ago [3], the use of secondary resonators (generally known as dynamic vibration absorbers) attached to a master structure to reduce vibration has been investigated for decades in the field of vibration and noise control engineering [23–28]. More recently, dynamic vibration absorbers have been implemented for the reduction of sound radiation from vibrating structures [29–31]. Some researchers also apply distributed vibration absorbers to improve the STL of thin structural partitions [32–35]. In their investigations a finite master structure is always specified and the resonance frequencies of the attached vibration absorbers are commonly tuned to some selected structural modes to suppress the structural vibration and in turn to reduce the sound transmission. Different constructions of distributed vibration absorbers have been proposed. In particular, Howard [35] considers the use of a regular array of beam-like vibration absorbers mounted on a thin plate. In his investigation [35], the beam-like absorbers are all tuned to slightly different natural frequencies and they are modeled as single degree of freedom spring–mass resonators. In contrast, Kidner et al. [33,45] and Idrisi et al. [34,46] develop the idea of using heterogeneous blankets attached to a thin plate. Such heterogeneous blankets are made of poro-elastic layers with embedded masses, and they are commonly treated as an array of spring–mass resonators to simplify the modeling and design process [33,34,45,46].

In the present work, we study the STL of an infinite locally resonant thin plate consisting of multiple subwavelength arrays of spring–mass resonators attached to an unbounded homogenous thin plate. As an analogue to acoustic metamaterials, we regard such locally resonant plate systems as metamaterial-based thin plates. Elastic wave propagation in metamaterial-based thin plates with periodic arrays of stepped resonant structures has been examined recently [14,16–18]. However, the sound transmission behavior of such structures has received little attention. The present work is intended to develop and expand the properties of metamaterial-based plates. One purpose is to reveal the opportunities of such structures to improve the STL of a thin plate at frequencies within the mass-law region and the coincidence region of sound transmission. Another purpose is to examine the potential of using extremely thin plates to construct metamaterial-based plates as low-frequency sound insulation materials.

2. The model and the method

In this section two analytical methods are developed for the problem. The first one is the so-called plane wave expansion (PWE) method. In the area of phononic crystals, PWE formulations are well developed for the study of wave propagation and transmission in two-dimensional (2D) and 3D periodic inhomogeneous medium with various types of periodic lattices [15,36,37]. On the other hand, PWE method is also known as the space-harmonics approach in the field of structural acoustics, where uniform plates with periodic supports or stiffeners are commonly considered [38–43]. Here, we extend the PWE method to treat the sound transmission problem of a locally resonant thin plate with 2D multiple periodic arrays of attached resonators. In the PWE formulations developed here there are no restrictions on the lattice type of the resonator arrays and the location of resonators.

The second one is an effective medium method. Effective medium theory is broadly developed for the study of acoustic metamaterials recently [4,6,7]. Knowing the effective medium parameters of a metamaterial is useful for predicting and understanding the global wave behavior of the metamaterial. Moreover, the effective medium theory has been shown to provide helpful guidance in designing acoustic metamaterials with desired properties [44]. For the locally resonant plate systems considered here, if the lattice constant of the resonator arrays is much smaller (i.e. in a subwavelength region) than the wavelength of the motion in the plate, we may treat such a plate-resonator coupled system as a metamaterial-based plate with effective dynamic mass density. Then the problem can be simplified significantly. Such an idea is similar to the treatments developed in the study of locally resonant acoustic metamaterials containing subwavelength arrays of embedded resonant units [6,7].

Although the PWE method can be employed to study resonator arrays in general, in the present work we focus on the subwavelength case. More general cases are deferred to future work. The PWE method is proposed here as a benchmark model to verify the validity of the effective medium method.

2.1. General case: PWE method

Consider an infinite thin plate, lying in the x–y plane, which has 2D periodic arrays of spring–mass resonators attached to it as shown in Fig. 1(a). Such a system can be considered as a simplified physical model of the two practical constructions sketched in Fig. 1(b) and (c). The construction illustrated in Fig. 1(b) represents a periodic extension of the system reported by Howard [35], while that sketched in Fig. 1(c) comes from work of Kidner et al. [33,45] and Idrisi et al. [34,46]. In the present work, we only address the simplified model shown in Fig. 1(a) to emphasize the central physical ideas.

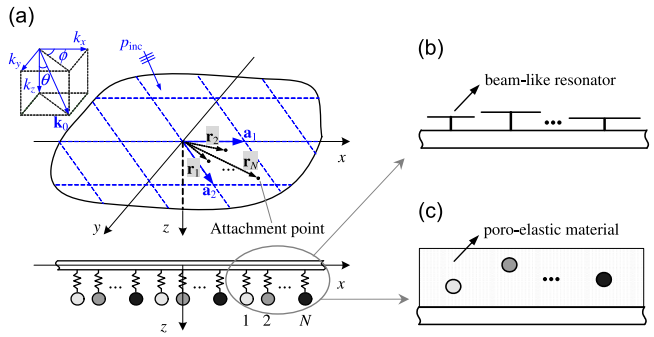

Fig. 1. (a) Schematic diagram of an infinite locally resonant thin plate with 2D multiple periodic arrays of attached spring–mass resonators; (b) and (c) sketch two practical constructions (side view of one unit cell) of the system shown in (a).

For the system shown in Fig. 1(a), in general there are N resonators attached in each unit cell. The spring constant and mass of the jth resonator in each unit cell are $k_{r,j}$ and $m_{r,j}$. Damping is introduced by means of a complex spring constant, i.e., $k_{r,j}\rightarrow k_{r,j}(1+\mathrm{i}\eta_{r,j})$, where $\eta_{r,j}$ is the loss factor. The attachment point of each resonator is denoted by the vector:

$$\mathbf{r}_j+\mathbf{R}=\mathbf{r}_j+(\overline{m}\mathbf{a}_1+\overline{n}\mathbf{a}_2), \tag{1}$$

where $\mathbf{r}_j=(x_j, y_j)$ represents the location of the jth resonator in the unit cell depicted in Fig. 1, $\overline{m}$ and $\overline{n}$ are integers, $\mathbf{a}_1=(a_{1x}, a_{1y})$ and $\mathbf{a}_2=(a_{2x}, a_{2y})$ are basis vectors of the direct lattice [15,47].

Assume an oblique plane sound wave (p_{inc}) varying harmonically in time is incident upon the plate with elevation angle θ and azimuth angle ϕ. The amplitude of the incident wave is P_0, and the associated sound wavenumber vector $\mathbf{k}_0$ can be decomposed in the x, y and z-direction:

$$p_{\mathrm{inc}}(x,y,z,t)=P_{\mathrm{inc}}(x,y,z)\mathrm{e}^{\mathrm{i}\omega t}=P_0\mathrm{e}^{-\mathrm{i}(k_x x+k_y y+k_z z)}\mathrm{e}^{\mathrm{i}\omega t}, \tag{2}$$

where

$$k_x=k_0\sin\theta\cos\phi,\quad k_y=k_0\sin\theta\sin\phi,\quad k_z=k_0\cos\theta,\quad k_0=\omega/c_0, \tag{3}$$

where c_0 is the sound speed in air. Let $\mathbf{r}=(x, y)$ and $\mathbf{k}=(k_x, k_y)$, then the incident sound pressure can be written as

$$p_{\mathrm{inc}}(\mathbf{r},z,t)=P_0\mathrm{e}^{-\mathrm{i}\mathbf{k}\cdot\mathbf{r}}\mathrm{e}^{-\mathrm{i}k_z z}\mathrm{e}^{\mathrm{i}\omega t}. \tag{4}$$

The plate vibrates harmonically and creates reflected and transmitted sound waves in the upper and lower half-space, respectively. Accordingly, the governing equation for the vibration of the thin plate takes the following form:

$$\begin{aligned}D\nabla^4 w(\mathbf{r})-\rho h\omega^2 w(\mathbf{r})&=p_{\mathrm{inc}}(\mathbf{r},z)_{z=0}+p_{\mathrm{ref}}(\mathbf{r},z)_{z=0}-p_{\mathrm{tr}}(\mathbf{r},z)_{z=0}\\&+\sum_{j=1}^{N}\sum_{\mathbf{R}}f_j(\mathbf{r}_j+\mathbf{R})\delta[\mathbf{r}-(\mathbf{r}_j+\mathbf{R})],\end{aligned} \tag{5}$$

where the time dependence $\exp(\mathrm{i}\omega t)$ is suppressed, $\nabla^4=(\partial^2/\partial x^2+\partial^2/\partial y^2)^2$, $w(\mathbf{r})$ represents the transverse displacement of the plate, p_{ref} and p_{tr} are the reflected and transmitted sound pressure. In addition, $D=Eh^3/12(1-\nu^2)$ is the plate bending stiffness, E, ν and ρ are the Young's modulus, Poisson's ratio and mass density of the plate material, h is the thickness of the plate. Damping is taken into account by introducing a complex Young's modulus, $E(1+\mathrm{i}\eta_p)$, where η_p is the loss factor of the plate material. In the last summation term of Eq. (5), $f_j(\mathbf{r}_j+\mathbf{R})$ refers to the force applied to the plate by the resonator locating at $\mathbf{r}_j+\mathbf{R}$, and $\delta[\mathbf{r}-(\mathbf{r}_j+\mathbf{R})]$ is a two dimensional delta function defined by

$$\delta[\mathbf{r}-(\mathbf{r}_j+\mathbf{R})]=\delta[x-(\mathbf{r}_j+\mathbf{R})_x]\delta[y-(\mathbf{r}_j+\mathbf{R})_y]. \tag{6}$$

Due to the periodicity of the locally resonant plate system, the displacement response of the plate can be written as [15,36]

$$w(\mathbf{r})=\sum_{\mathbf{G}}W_{\mathbf{G}}\mathrm{e}^{-\mathrm{i}(\mathbf{k}+\mathbf{G})\cdot\mathbf{r}}. \tag{7}$$

Here, $\mathbf{G}$ denotes the reciprocal-lattice vector [15,47], given by

$$\mathbf{G}=m\mathbf{b}_1+n\mathbf{b}_2, \tag{8}$$

where m and n are integers, $\mathbf{b}_1=(b_{1x}, b_{1y})$ and $\mathbf{b}_2=(b_{2x}, b_{2y})$ are basis vectors of the reciprocal lattice, which are defined such that [15,47]

$$\mathbf{a}_p\cdot\mathbf{b}_q=2\pi\delta_{pq}\quad(p,q=1,2). \tag{9}$$

Thus, the expanded form of Eq. (7) is given by

$$w(x,y)=\sum_{m=-\infty}^{\infty}\sum_{n=-\infty}^{\infty}W_{mn}\mathrm{e}^{-\mathrm{i}(k_x+mb_{1x}+nb_{2x})x}\mathrm{e}^{-\mathrm{i}(k_y+mb_{1y}+nb_{2y})y}. \tag{10}$$

Similar to Eq. (7), the reflected and transmitted sound pressures can be expressed by

$$p_{\mathrm{ref}}(\mathbf{r},z)=\sum_{\mathbf{G}}P_{\mathrm{ref},\mathbf{G}}\mathrm{e}^{-\mathrm{i}(\mathbf{k}+\mathbf{G})\cdot\mathbf{r}}\mathrm{e}^{+\mathrm{i}k_{z,\mathbf{G}}z}, \tag{11}$$

$$p_{\mathrm{tr}}(\mathbf{r},z)=\sum_{\mathbf{G}}P_{\mathrm{tr},\mathbf{G}}\mathrm{e}^{-\mathrm{i}(\mathbf{k}+\mathbf{G})\cdot\mathbf{r}}\mathrm{e}^{-\mathrm{i}k_{z,\mathbf{G}}z}, \tag{12}$$

where

$$k_{z,\mathbf{G}}=\begin{cases}\sqrt{k_0^2-|\mathbf{k}+\mathbf{G}|^2}; & k_0^2\geq|\mathbf{k}+\mathbf{G}|^2,\\ -\mathrm{i}\sqrt{|\mathbf{k}+\mathbf{G}|^2-k_0^2}; & k_0^2<|\mathbf{k}+\mathbf{G}|^2.\end{cases} \tag{13}$$

Note that the forces exerted on the plate by the resonators also satisfy the periodic condition, i.e.,

$$f_j(\mathbf{r}_j+\mathbf{R})=f_j(\mathbf{r}_j)\mathrm{e}^{-\mathrm{i}\mathbf{k}\cdot\mathbf{R}}. \tag{14}$$

Hence the resonator force term in Eq. (5) can be reformulated as

$$\sum_{\mathbf{R}}f_j(\mathbf{r}_j+\mathbf{R})\delta[\mathbf{r}-(\mathbf{r}_j+\mathbf{R})]=f_j(\mathbf{r}_j)\mathrm{e}^{-\mathrm{i}\mathbf{k}\cdot(\mathbf{r}-\mathbf{r}_j)}\sum_{\mathbf{R}}\delta[\mathbf{r}-(\mathbf{r}_j+\mathbf{R})]. \tag{15}$$

Now introduce a function defined by $g(\mathbf{r})=\sum_{\mathbf{R}}\delta[\mathbf{r}-(\mathbf{r}_j+\mathbf{R})]$. Due to the periodicity of this function, it can be expressed in Fourier series as [18]

$$g(\mathbf{r})=\sum_{\mathbf{G}}\frac{1}{S}\mathrm{e}^{\mathrm{i}\mathbf{G}\cdot\mathbf{r}_j}\mathrm{e}^{-\mathrm{i}\mathbf{G}\cdot\mathbf{r}}, \tag{16}$$

where $S=|\mathbf{a}_1\times\mathbf{a}_2|$ is the area of the unit cell associated with the periodic lattice. Combining Eqs. (15) and (16) yields the following relation:

$$\sum_{\mathbf{R}}f_j(\mathbf{r}_j+\mathbf{R})\delta[\mathbf{r}-(\mathbf{r}_j+\mathbf{R})]=f_j(\mathbf{r}_j)\frac{1}{S}\sum_{\mathbf{G}}\mathrm{e}^{i(\mathbf{k}+\mathbf{G})\cdot\mathbf{r}_j}\mathrm{e}^{-i(\mathbf{k}+\mathbf{G})\cdot\mathbf{r}}. \tag{17}$$

By analyzing time-harmonic vibration of the resonators, it can be found that the force $f_j(\mathbf{r}_j)$ is related to the plate displacement $w(\mathbf{r}_j)$ by [18]

$$f_j(\mathbf{r}_j)=-D_{r,j}w(\mathbf{r}_j), \tag{18}$$

where

$$D_{\mathrm{r},j}=\frac{-\omega^2m_{r,\,j}}{1-\omega^2/[\omega_{r,\,j}^2(1+\mathrm{i}\eta_{r,\,j})]} \tag{19}$$

is the dynamic stiffness of the jth resonator, and $\omega_{r,\,j}=(k_{r,\,j}/m_{r,\,j})^{1/2}=2\pi f_{r,\,j}$ represents the resonance frequency of the resonator.

At the air–plate interfaces, the continuity conditions of normal velocity require that

$$\frac{\partial[p_{\mathrm{inc}}(\mathbf{r},z)+p_{\mathrm{ref}}(\mathbf{r},z)]}{\partial z}|z=0=\rho_0\omega^2w(\mathbf{r}), \tag{20}$$

$$\frac{\partial[p_{\mathrm{tr}}(\mathbf{r},z)]}{\partial z}|z=0=\rho_0\omega^2w(\mathbf{r}). \tag{21}$$

Substituting Eqs. (4), (7), (11) and (12) into Eqs. (20) and (21) and requiring the sums to be true for all choices of $\mathbf{r}$, the sound pressure coefficients and plate displacement coefficients are related for each $\mathbf{G}$:

$$P_{\mathrm{ref},\mathbf{G}}=P_0\delta_{\mathbf{0}-\mathbf{G}}-\frac{\mathrm{i}\rho_0\omega^2}{k_{z,\mathbf{G}}}W_{\mathbf{G}}, \tag{22}$$

$$P_{\mathrm{tr},\mathbf{G}}=\frac{\mathrm{i}\rho_0\omega^2}{k_{z,\mathbf{G}}}W_{\mathbf{G}}, \tag{23}$$

where

$$\delta_{\mathbf{0}-\mathbf{G}}=\begin{cases}1, & \mathbf{G}=\mathbf{0},\\ 0, & \mathbf{G}\neq\mathbf{0}.\end{cases} \tag{24}$$

Inserting Eqs. (4), (7), (11), (12) and (17) into the governing equation (5) and considering that the equation holds for all possible choices of $\mathbf{r}$, the following relationship is obtained:

$$\left\{DS[(\mathbf{k}+\mathbf{G})_x^2+(\mathbf{k}+\mathbf{G})_y^2]^2+\mathrm{i}\omega(2\rho_0\omega S/k_{z,\mathbf{G}})-\omega^2\rho hS\right\}W_{\mathbf{G}}$$

$$+\sum_{j=1}^{N}\sum\nolimits_{\mathbf{G}'}D_{r,j}\mathrm{e}^{\mathrm{i}\mathbf{G}\cdot\mathbf{r}_j}\mathrm{e}^{-\mathrm{i}\mathbf{G}'\cdot\mathbf{r}_j}W_{\mathbf{G}'}=2P_0S\delta_{\mathbf{0}-\mathbf{G}}. \tag{25}$$

This represents an infinite set of linear equations. In practice, a finite number of reciprocal-lattice vectors are taken into account for the numerical calculation. If we choose $m=n=(-M,\ \ldots,\ M)$ for the assignment of the reciprocal-lattice vectors $\mathbf{G}$ and $\mathbf{G}'$, the number of plane waves ($W_{\mathbf{G}}$) used in the calculation is $\overline{N}=(2M+1)^2$. Then Eq. (25) can be expressed in a matrix form as

$$([\mathbf{K}_\mathrm{p}]+\mathrm{i}\omega[\mathbf{C}_\mathrm{f}]-\omega^2[\mathbf{M}_\mathrm{p}]+[\mathbf{D}_\mathrm{r}])\{\mathbf{W}_{\mathbf{G}}\}=2P_0S\{\boldsymbol{\delta}_{\mathbf{0}-\mathbf{G}}\}, \tag{26}$$

where $\mathbf{K}_p$ and $\mathbf{M}_p$ are plate stiffness and mass matrices, $\mathbf{C}_f$ is fluid loading matrix, and $\mathbf{D}_r$ is dynamic stiffness matrix of the resonators. The expanded forms of the matrices and vectors in Eq. (26) are detailed in Appendix.

Eq. (26) provides a straightforward way for the calculation of displacement coefficients $W_{\mathbf{G}}$ for general case of resonator arrays. If we consider the case of a single array of resonators (with $N=1$ and $\mathbf{r}_1=\mathbf{0}$), the problem can be further simplified, since Eq. (25) can be written as

$$W_{\mathbf{G}}=2P_0S\Delta_{\mathbf{0}}\delta_{\mathbf{0}-\mathbf{G}}-D_{r,1}\Delta_{\mathbf{G}}\sum\nolimits_{\mathbf{G}'}W_{\mathbf{G}'}, \tag{27}$$

where

$$\Delta_{\mathbf{G}}=\{DS[(\mathbf{k}+\mathbf{G})_x^2+(\mathbf{k}+\mathbf{G})_y^2]^2+\mathrm{i}\omega(2\rho_0\omega S/k_{z,\mathbf{G}})-\omega^2\rho hS\}^{-1}. \tag{28}$$

Note that Eq. (27) suggests

$$\sum_{\mathbf{G}}W_{\mathbf{G}}=\sum_{\mathbf{G}}[2P_0S\Delta_{\mathbf{0}}\delta_{\mathbf{0}-\mathbf{G}}-D_{\mathrm{r},1}\Delta_{\mathbf{G}}(\sum\nolimits_{\mathbf{G}'}W_{\mathbf{G}'})]. \tag{29}$$

Thus the infinite sum of the displacement coefficients can be obtained as

$$\sum_{\mathbf{G}}W_{\mathbf{G}}=\frac{2P_0S\Delta_{\mathbf{0}}}{1+D_{r,1}\sum_{\mathbf{G}'}}\Delta_{\mathbf{G}'}. \tag{30}$$

Substituting this into Eq. (27) gives an explicit solution of the displacement coefficients:

$$W_{\mathbf{G}}=2P_0S\Delta_{\mathbf{0}}\left[\delta_{\mathbf{0}-\mathbf{G}}-\frac{\Delta_{\mathbf{G}}}{(1/D_{r,1})+\sum_{\mathbf{G}'}}\Delta_{G'}\right]. \tag{31}$$

Once the plate displacement coefficients $W_{\mathbf{G}}$ are known, we can find the sound pressure coefficients by using Eqs. (22) and (23). It should be pointed out that, among the infinite components of the transmitted pressure involved in Eq. (12), only those taking a real wavenumber in the z-direction could radiate energy, and the total transmitted sound power is equal to the sum of the powers transmitted by each of such component. Thus the oblique sound power transmission coefficient is

$$\tau_p(\theta,\phi)=\frac{\sum_{\mathbf{G}}|P_{\mathrm{tr},\mathbf{G}}|^2\mathrm{Re}(k_{z,\mathbf{G}})}{|P_0|^2k_z}. \tag{32}$$

The diffuse field power transmission coefficient [48] is then obtained by averaging the oblique transmission coefficient over the elevation angle θ and azimuth angle ϕ:

$$\tau_{\mathrm{diff}}=\frac{\int_0^{2\pi}\int_0^{\pi/2}\tau_p(\theta,\phi)\sin\theta\cos\theta\,\mathrm{d}\theta\,\mathrm{d}\phi}{\int_0^{2\pi}\int_0^{\pi/2}\sin\theta\cos\theta\,\mathrm{d}\theta\,\mathrm{d}\phi}=\frac{2}{\pi}\int_0^{\pi}\int_0^{\pi/2}\tau_p(\theta,\phi)\sin\theta\cos\theta\,\mathrm{d}\theta\,\mathrm{d}\phi. \tag{33}$$

The formulations derived above hold for various types of lattice for the resonator array. However, in this paper, we only consider the square lattice as an example case. The basis vectors of a square lattice can be written as $\mathbf{a}_1=(a,\ 0)$ and $\mathbf{a}_2=(0,\ a)$, where a is the lattice constant, and the basis vectors of the corresponding reciprocal lattice are $\mathbf{b}_1=(2\pi/a,\ 0)$, $\mathbf{b}_2=(0,\ 2\pi/a)$. Taking into account the symmetry of the periodic lattice, the diffuse field power transmission coefficient can be written as

$$\tau_{\mathrm{diff}}=\frac{8}{\pi}\int_0^{\pi/4}\int_0^{\pi/2}\tau_p(\theta,\phi)\sin\theta\cos\theta\,\mathrm{d}\theta\,\mathrm{d}\phi. \tag{34}$$

The oblique or diffuse field sound transmission loss (STL) [48] is defined by

$$\mathrm{STL} = 10\log_{10}\left(\frac{1}{\tau}\right), \tag{35}$$

where the transmission coefficient τ is obtained from Eqs. (32), (33) or (34).

2.2. Subwavelength case: effective medium method

For the subwavelength case of resonator arrays, we treat the locally resonant plate shown in Fig. 1(a) as a metamaterial-based plate with effective dynamic mass density. The effective dynamic mass density can be obtained by two steps. First, let the jth resonator be replaced by an equivalent mass $m_{\mathrm{equiv},\,j}$ attached solidly to the plate such that

$$m_{\mathrm{equiv},\,j} = \frac{m_{r,\,j}}{1-\omega^2/[\omega_{r,\,j}^2(1+\mathrm{i}\eta_{r,\,j})]}. \tag{36}$$

The undamped form (i.e., $\eta_{rj}=0$) of the expression (36) can be found in the classic textbook [23] by Den Hartog when discussing the dynamic vibration absorbers. Den Hartog also pointed out that the equivalent mass is positive for low frequencies, is infinitely large at the resonance frequency $\omega_{r,\,\mathrm{j}}$, and is negative for high frequencies [23].

Next, we average each equivalent mass over one unit cell of the periodic system, so that the effective dynamic mass density of the metamaterial-based plate can be written as

$$\rho_{\mathrm{eff}}(\omega) = \left(\rho Sh + \sum_{j=1}^{N} m_{\mathrm{equiv},\,j}\right)\frac{1}{Sh} = \rho + \sum_{j=1}^{N}\frac{\rho_{r,\,j}}{1-\omega^2/[\omega_{r,\,j}^2(1+\mathrm{i}\eta_{r,\,j})]}, \tag{37}$$

where $\rho_{r,\,j} = m_{r,\,j}/Sh$, S is the surface area of one unit cell, and N represents the total number of resonators attached in one unit cell. Eq. (37) indicates that the effective dynamic mass density is frequency dependent, and it is different from the static mass density of the metamaterial-based plate, which is given by

$$\rho_{\mathrm{st}} = \left(\rho Sh + \sum_{j=1}^{N} m_{r,\,j}\right)\frac{1}{Sh} = \rho + \sum_{j=1}^{N}\rho_{r,\,j}. \tag{38}$$

For convenience of description, we define the mass ratio of the resonators as

$$\gamma = \sum_{j=1}^{N} m_{\mathrm{r},\,j}/\rho Sh = \sum_{j=1}^{N}\rho_{\mathrm{r},\,j}/\rho. \tag{39}$$

By using the effective dynamic mass density ρ_{eff}, the flexural wavenumber of the metamaterial-based plate can be obtained by

$$k_{p,\mathrm{eff}}^4 = \rho_{\mathrm{eff}}h\omega^2/D, \tag{40}$$

and the sound transmission problem can be modeled simply in the same way as for a bare plate, i.e.,

$$D\nabla^4 w(\mathbf{r}) - \rho_{\mathrm{eff}}h\omega^2 w(\mathbf{r}) = p_{\mathrm{inc}}(\mathbf{r},z)_{z=0} + p_{\mathrm{ref}}(\mathbf{r},z)_{z=0} - p_{\mathrm{tr}}(\mathbf{r},z)_{z=0}. \tag{41}$$

By assuming plane wave solutions for the plate displacement and sound pressures, and considering the continuity condition of fluid–structure coupling, the oblique sound power transmission coefficient can be obtained as

$$\tau_p(\theta,\phi) = \tau_p(\theta) = \left|\frac{2\rho_0 c_0\omega}{\Delta(\omega)\cos\theta}\right|^2, \tag{42}$$

where

$$\Delta(\omega) = D(k_0\sin\theta)^4 - \rho_{\mathrm{eff}}h\omega^2 + 2\mathrm{i}\rho_0 c_0\omega/\cos\theta. \tag{43}$$

The diffuse field power transmission coefficient is then calculated by [48]

$$\tau_{\mathrm{diff}} = \frac{\int_0^{\pi/2}\tau_p(\theta)\sin\theta\cos\theta\,\mathrm{d}\theta}{\int_0^{\pi/2}\sin\theta\cos\theta\,\mathrm{d}\theta} = \int_0^{\pi/2}\tau_p(\theta)\sin 2\theta\,\mathrm{d}\theta. \tag{44}$$

The corresponding STL can be calculated by Eq. (35).

3. Thin plates

We initially consider thin plates similar in thickness to the existing plates or plate-like structures that are commonly used in engineering. Prevention of sound transmission through such plate structures is particularly important in systems such as aircraft [34], buildings [49], and launch vehicles [32,33]. It is well known that air-borne sound transmission through an unbounded thin plate is commonly characterized by three different frequency regions: the mass-law region

(well below the coincidence frequency ω_{co}), the coincidence region (around ω_{co}) and the stiffness control region (well above ω_{co}) [48]. In the mass-law region, the STL is determined primarily by surface mass density (mass per unit area) of the plate, and in the coincidence region, both the mass and the damping dominate the STL [48]. It is also known that lightweight, stiff plate-like partitions tend to exhibit lower coincidence frequencies [48]. Accordingly, the design of lightweight plates or plate-like partitions with high STL at low frequencies remains a challenging problem.

In this section, we will demonstrate that the STL of a metamaterial-based thin plate (taking a 4 mm thick aluminum plate as an example) can deviate significantly from that of a bare plate, which shows some opportunities to improve the sound insulation performance of thin plates in the mass law region as well as in the coincidence region. In what follows, these two characteristic regions will be addressed separately.

3.1. Tuned to the mass law region

We first examine the case that the resonance frequency of the resonators is tuned to the mass law region. At the beginning, we consider that only a single array of resonators ($N=1$ and $\mathbf{r}_1=\mathbf{0}$) is involved in the metamaterial-based plate. The properties of the metamaterial-based plate are listed in Table 1, where $\eta_{r,1}$ and $f_{r,1}$ are written as η_r and f_r for brevity. The properties of air are $\rho_0=1.2$ kg/m^3 and $c_0=340$ m/s. In addition, we assume that the resonators are attached in a square array with a lattice constant ($a=0.035$ m) much smaller than the flexural wavelength [$\lambda_p=2\pi(D/\rho h\omega^2)^{1/4}$] of the host plate at the resonance frequency ($f_r=300$ Hz). The ratio a/λ_p is calculated to be 0.1 at the frequency f_r, which confirms the subwavelength assumption for the resonator array.

Fig. 2(a) shows the oblique STL of the metamaterial-based plate for a sound wave incident at $\phi=0$ and $\theta=\pi/3$. Both the predictions by the plane wave expansion (PWE) method and the effective medium method are presented, which show very good agreement with each other. It should be noted that the effective medium method can be performed with much less

Table 1
Properties of a metamaterial-based plate.

ρ	E	η_p	v	h	a	γ	η_r	f_r
2700 kg/m^3	70 GPa	0.005	0.33	0.004 m	0.035 m	0.2	0.005	300 Hz

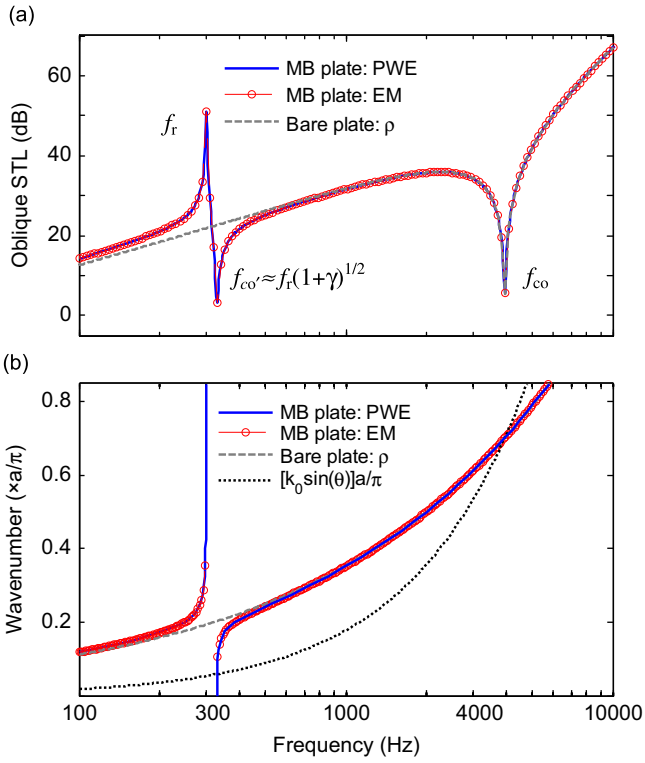

Fig. 2 (. a) The oblique STL and (b) the wavenumbers of a metamaterial-based (MB) plate and a bare plate. The acronyms MB and EM refer to "metamaterial-based" and "effective medium", respectively. The term $k_0 \sin(\theta)$ represents the trace wavenumber of the incident sound wave ($\phi=0$ and $\theta=\pi/3$).

effort than the PWE method. In Fig. 2(a), the STL of the bare plate are also presented for comparison. It can be seen that the metamaterial-based plate and the bare plate display the same behavior in the high frequency range ($f \gg f_r$), where a significant drop on the STL curve is observed. This is due to the well-known coincidence phenomenon. For a sound wave incident at θ, the coincidence frequency is given by [48]

$$f_{co}(\theta) = \left(\frac{c_0}{\sin\theta}\right)^2 \sqrt{\frac{\rho h}{D}}, \tag{45}$$

The lowest coincidence frequency is known as the critical frequency:

$$f_c = c_0^2 \sqrt{\frac{\rho h}{D}}. \tag{46}$$

For the plate considered here, by using Eqs. (45) and (46) we can obtain that $f_{co}(\pi/3) = 3938$ Hz, and $f_c = 2954$ Hz. This confirms that the resonance frequency f_r (=300 Hz) is tuned to the mass law region (i.e.$f_r \ll f_{co}$).

Fig. 2(a) clearly indicates that the STL curve of the metamaterial-based plate deviates a lot from that of the bare plate in a frequency range around the resonance frequency f_r. In particular, a striking peak arises at the resonance frequency f_r, and a noticeable dip appears at a somewhat higher frequency $f_{co'}$. To understand the dip frequency, the dispersion relations of the metamaterial-based plate and the bare plate as well as the trace wavenumber [$k_0 \sin(\theta)$] of the incident sound wave are presented in Fig. 2(b). It is seen that the PWE method [18] (calculated by Eq. (26) with $P_0 = 0$ and $\mathbf{C}_f = \mathbf{0}$) and the effective medium method (Eq. (40)) give almost identical results. It can be also seen that a band gap exists in the metamaterial-based plate. The lower and upper edge frequencies of this band gap can be well approximated by the frequencies f_r and $f_r(1+\gamma)^{1/2}$, respectively, which is very similar to other locally resonant systems [10,50]. Furthermore, the intersections of the wavenumber curve of the metamaterial-based plate and the trace wavenumber curve of the incident sound wave explain exactly the location of the two STL dips shown in Fig. 2(a). The results suggest that, for the metamaterial-based plate, an additional low-frequency coincidence condition exists, and the lower coincidence frequency $f_{co'}$ can be well approximated by the upper gap edge frequency, i.e., $f_{co'} \approx f_r(1+\gamma)^{1/2}$, since the dispersion relation of the metamaterial-based plate is rather flat around the upper gap edge.

In order to gain a further insight into the unique STL of the metamaterial-based plate, in Fig. 3(a) we compare the three types of mass density: ρ_{eff}, ρ_{st} and ρ. It is shown that the effective mass density of the metamaterial-based plate ρ_{eff} is infinite large at the resonance frequency f_r, but is zero at the frequency $f_r(1+\gamma)^{1/2}$, and is negative in the frequency range $f_r < f < f_r(1+\gamma)^{1/2}$. At frequencies below the resonance frequency f_r, ρ_{eff} is generally larger than the static mass density ρ_{st},

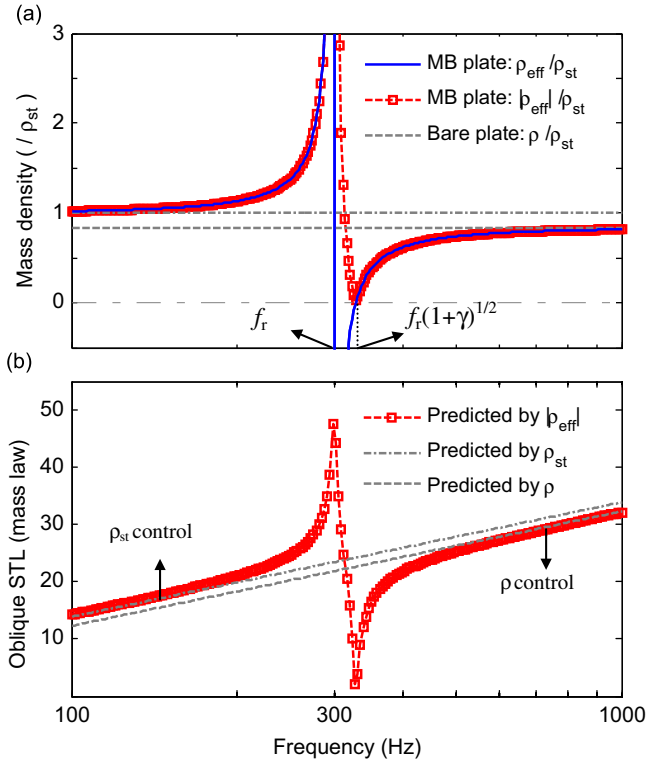

Fig. 3. (a) The mass density and (b) the oblique STL of a metamaterial-based (MB) plate and two bare plates. The results in (b) are predicted by the mass-law equation (48).

but at low enough frequencies, ρ_{eff} approaches ρ_{st}. On the other hand, at frequencies above the frequency $f_r(1+\gamma)^{1/2}$, ρ_{eff} is always smaller than the bare plate density ρ, but at high enough frequencies, ρ_{eff} approaches ρ. Such comparisons can help us understand the characteristics of STL of different plate systems. We know that, for a bare plate, the oblique sound power transmission coefficient at frequencies well below the critical frequency can be well approximated by [48]

$$\tau(\theta) = 1/[1+(\omega\rho h\cos\theta/2\rho_0 c_0)^2]. \tag{47}$$

It is normally true that $\omega|\rho|h\cos\theta \gg 2\rho_0 c_0$, thus Eq. (47) yields the well-known obliquely incident mass law:

$$\text{STL}(\theta) = 20\log_{10}(\omega|\rho|h\cos\theta/2\rho_0 c_0). \tag{48}$$

By substituting the expression of ρ_{eff} into Eq. (48), we obtain an approximation of the STL of the metamaterial-based plate, as shown in Fig. 3(b). The results generally match well with those shown in Fig. 2(a), but some discrepancy occurs around the frequency $f_r(1+\gamma)^{1/2}$. This is because ρ_{eff} is zero at this frequency, thus the assumption $\omega|\rho|h\cos\theta \gg 2\rho_0 c_0$is not true. In general, the thinner the plate is the greater the discrepancy would be. By using mass law eq. (48), we also predict the STL of two bare plates, with the mass density ρ_{st} and ρ, respectively. As expected, at low enough frequencies the STL of the metamaterial-based plate is controlled by ρ_{st}, but at high enough frequencies (still within the mass law region) it is controlled by ρ (see Fig. 3(b)).

Fig. 4(a) shows the evolution of the oblique STL of the metamaterial-based plate with varying incident angle θ. The STL always decreases with increasing θ, but the locations of the peak and dip in the STL curves remain unchanged. Fig. 4(b) shows the diffuse field STL of the metamaterial-based plate predicted by the PWE method, together with that predicted by the effective medium method. Very good agreement between the two methods is seen again. For a comparison, the diffuse field STL curves of two bare plates (with the mass density ρ_{st} or ρ) are also presented in Fig. 4(b). The comparison indicates that the metamaterial-based plate can result in STL much higher than merely increasing the mass density of the plate, which is similar to increasing the thickness of the plate. However, the increase of STL by the metamaterial-based plate only results in a narrow frequency band around the resonance frequency f_r. At frequencies immediately higher than f_r, the STL of the metamaterial-based plate is always lower than that of a bare plate with the same surface mass density (i.e. $\rho_{\text{st}}h$).

To broaden the operating bandwidth of a resonator, a well-known method is to divide the resonator mass between multiple detuned resonators [26,28]. Fig. 5 shows the diffuse field STL of metamaterial-based plates with a single or multiple resonators attached in each unit cell. The results are calculated by the effective medium method, whose validity is confirmed in previous examples. Here, the loss factor of the resonators is chosen as 0.05, and the combined mass ratio of the resonators is fixed to $\gamma = 0.2$ in each case. For the case of double resonators ($N=2$), the second resonance frequency $f_{r,2}$

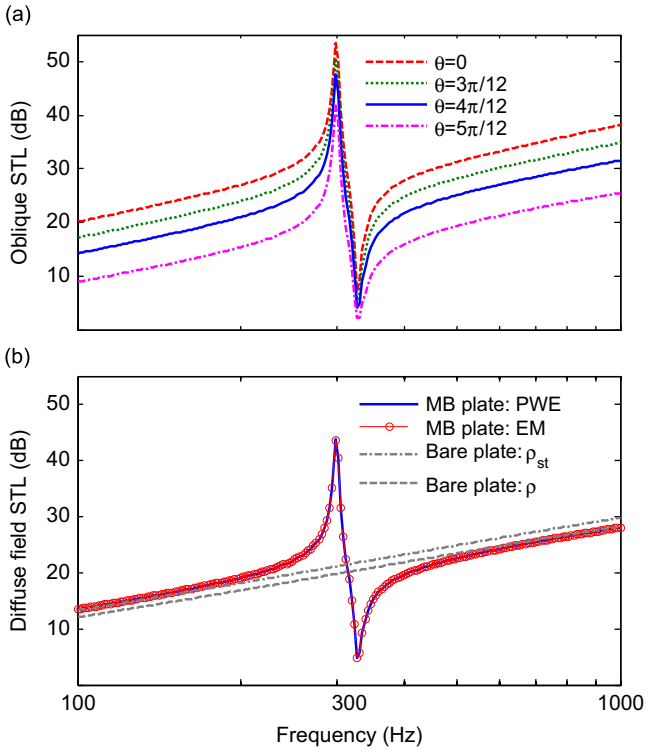

Fig. 4. (a) Evolution of the oblique STL of a metamaterial-based plate with changing incident angle θ. The azimuth angle is fixed at $\phi=0$. (b) Comparison of the diffuse field STL of the metamaterial-based plate and that of two bare plates. The acronyms MB and EM refer to "metamaterial-based" and "effective medium", respectively.

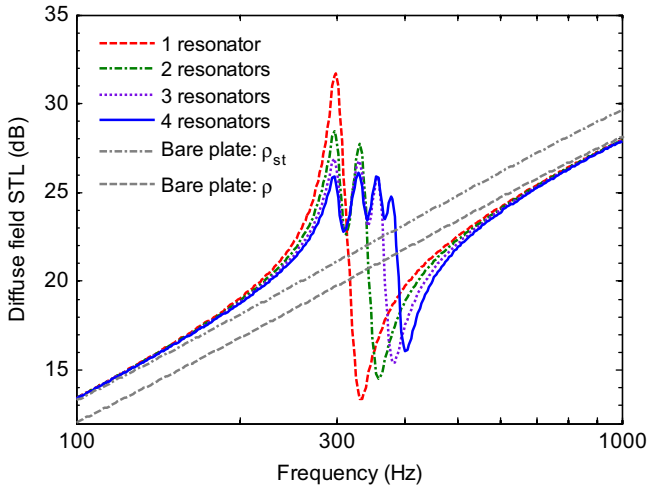

Fig. 5. Diffuse field STL of metamaterial-based plates with $N\,(=1, 2, 3, 4)$ attached resonators in each unit cell, $\eta_{r,j}=0.05$. The resonator parameters in the MB plates are chosen such that for $N=1$, $\gamma=m_r/\rho Sh=0.2$, and $f_r=300$ Hz; for $N=2$, $\gamma_j=m_{r,j}/\rho Sh=0.2/2$ $(j=1,2)$, and $(f_{r,1}, f_{r,2})=(300, 332)$ Hz; for $N=3$, $\gamma_j=0.2/3$ $(j=1,2,3)$, and $(f_{r,1}, f_{r,2}, f_{r,3})=(300, 332, 358)$ Hz; for $N=4$, $\gamma_j=0.2/4$ $(j=1, 2, 3, 4)$, and $(f_{r,1}, f_{r,2}, f_{r,3}, f_{r,4})=(300, 332, 358, 380)$ Hz.

is simply tuned to the dip frequency corresponding to the single resonator case. And similarly, for the case of triple resonators ($N=3$), the third resonance frequency $f_{r,3}$ is tuned to the dip frequency of the case of double resonators. This is followed in a similar way for the case of quadruple resonators. The results indicate two improvements achieved by the introduction of multiple detuned resonators. On the one hand, the width of the frequency band with increased STL is broadened a lot. On the other hand, the additional coincidence region (characterized by the STL dip) is narrowed and shifted to some higher frequency range with higher STL at the dip frequency. The performance of the case of multiple resonators may be further improved by increasing the number of resonators and using some optimization techniques to assign the resonator parameters, but these aspects are not addressed in the present paper.

3.2. Tuned to the coincidence region

Then we examine the case that the resonance frequency of the resonators is tuned to the coincidence region. The properties of the metamaterial-based plate are the same as in Table 1, except that the loss factors are now chosen as $\eta_p=\eta_r=0.01$, and the resonance frequency is tuned to $f_r=4000$ Hz, which is very close to the coincidence frequency $f_{co}(\pi/3)=3938$ Hz. Here, the ratio a/λ_p is calculated to be 0.35 at the resonance frequency f_r. Thus the subwavelength assumption still holds at the resonance frequency, but is not as strong as in the previous case.

Fig. 6(a) shows the oblique STL of the metamaterial-based plate for a sound wave incident at $\phi=0$ and $\theta=\pi/3$. Both the predictions by the PWE method and by the effective medium method are presented. Results show that the two methods generally yield similar results. However, the effective medium method cannot predict the high frequency ($f_{co'}$) coincidence phenomenon, which is due to the intersection of the trace wavenumber of incident sound wave and the subsidiary Bloch wavenumber [15] of the metamaterial-based plate, as illustrated in Fig. 6(b). In the PWE model, periodic structural conditions are well applied, thus a full description of the Bloch wavenumbers can be calculated. In contrast, when using the effective medium method, we assume that the metamaterial-based plate is isotropic thus no Bloch wave exists. It should be pointed out that the coincidence phenomenon observed at the frequency $f_{co'}$ in Fig. 6 depends on the resonator spacing, which is no longer small enough in comparison with the flexural wavelength of the plate. At this coincidence frequency, a subsidiary Bloch wave (a slower wave) is excited by the convected sound wave of equal wavenumber (equal velocity), and in turn can excite the primary Bloch wave (faster wave) that can radiate sound. Such a mechanism was firstly clarified by Mead [51]; a more elaborate discussion of this phenomenon can be found in Ref. [51].

The dispersion relations predicted by the PWE method, as shown in Fig. 6(b), also indicate that, along the direction $\phi=0$, a Bragg-type band gap appears around a frequency governed by the Bragg condition of the system [18]:

$$f_B(\phi)=\frac{1}{2\pi}\left(\frac{\pi}{a\cos\phi}\right)^2\sqrt{\frac{D}{\rho h}}, \tag{49}$$

which yields $f_B(0)=7987$ Hz. Furthermore, Eq. (49) also implies that the location of the directional Bragg gap will move to higher frequencies as the azimuth angle ϕ increasing from 0 to $\pi/4$. One can also expect that, if the lattice constant a is chosen to be small enough, the directional Bragg gap will disappear in the frequency range considered ($\lesssim 10$ kHz). Examples for the case of smaller lattice constants a are not considered further. We suppose that a metamaterial-based plate with a very small lattice constant could be difficult to realize in some practice, especially when multiple resonators are required to be attached in each unit cell.

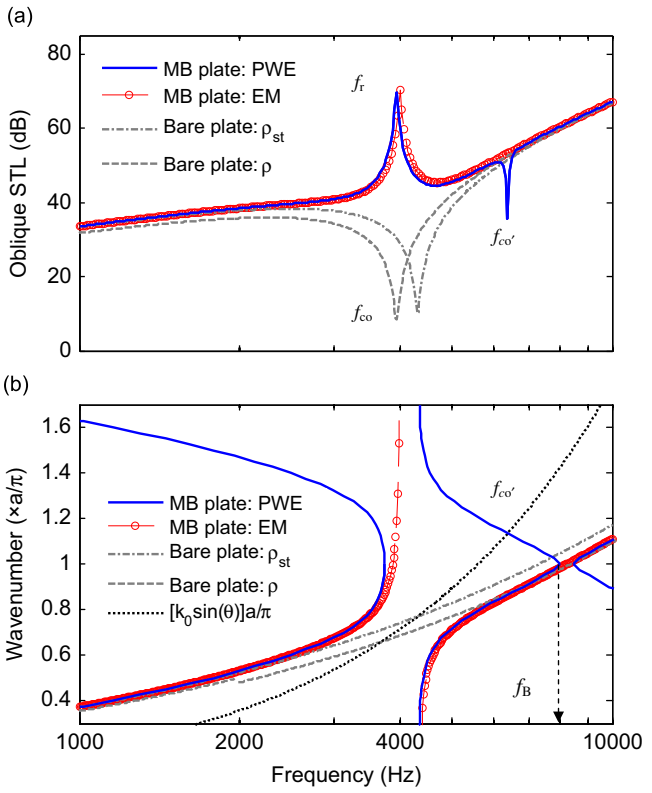

Fig. 6. (a) The oblique STL and (b) the wavenumbers of a metamaterial-based plate (f_r=4000 Hz) and two bare plates. In (b), $k_0 \sin(\theta)$ represents the trace wavenumber of the incident sound wave (ϕ=0,θ=π/3). The acronyms MB and EM refer to "metamaterial-based" and "effective medium", respectively.

The most interesting result in Fig. 6(a) is that the coincidence region of the bare plate is dramatically replaced by an anticoincidence region in the metamaterial-based plate, i.e., very high STL is achieved in a range around the coincidence frequency f_{co}. Particularly, the significant dip on the STL curve of the bare plate is replaced by a great peak on that of the metamaterial-based plate. Fig. 7(a) further shows that the great peak cannot be affected by changing the incident angle θ. This implies that such a high STL can also be achieved in the case of diffuse field sound incidence. This will be demonstrated later on. Fig. 7(a) also indicates that, although great STL is achieved around the traditional coincidence frequency f_{co}, some higher frequency dips do exist on the STL curves of the metamaterial-based plate, as denoted by the notations "A-F". Such dips can be well explained by the intersections between the wavenumber curve of the metamaterial-based plate and the trace wavenumber curves of different incident sound waves, as illustrated in Fig. 7(b). One can see that for the case of a smaller incident angle θ (e.g., $\theta < \pi/4$), two dips exist on the STL curve due to the existence of two coincidence conditions. In contrast, for the case of an appropriately large incident angle θ (e.g., $\theta = \pi/3$), the lower coincidence condition can be eliminated, and thus increased STL can be achieved in a wide band around the resonance frequency f_r.

Fig. 8 shows the diffuse field STL of the metamaterial-based plate predicted by the PWE method together with that calculated by the effective medium method. Good agreement is seen again. These results are compared with those of two bare plates with static mass density ρ_{st} and ρ, respectively. It is interesting to note that no visible coincidence region exists on the diffuse field STL curve of the metamaterial-based plate. In addition, extremely high STL is achieved in a region around the resonance frequency f_r.

Fig. 9 shows the evolution of the diffuse field STL of the metamaterial-based plate with varying resonance frequency f_r. It is seen that the benefit of the metamaterial-based plate can be always guaranteed by tuning the resonance frequency around or somewhat higher than the critical frequency f_c of the bare plate. If too low or too high resonance frequencies are chosen, a coincidence region with rather low STL may arise.

Fig. 10 shows the diffuse field STL of metamaterial-based plates with a single or multiple resonators attached in each unit cell. The idea is similar to that illustrated in Fig. 5. As previously, for each case, the loss factor of the resonators is chosen as 0.05, and the combined mass ratio of the resonators is $\gamma = 0.2$. It is seen that, by using multiple detuned resonators, the frequency band of improved STL is widened significantly. We also note that outside the improvement band the diffuse field STL of the metamaterial-based plate is almost the same as that of the bare plate with the same surface mass, this is very different from the case shown in Fig. 5.

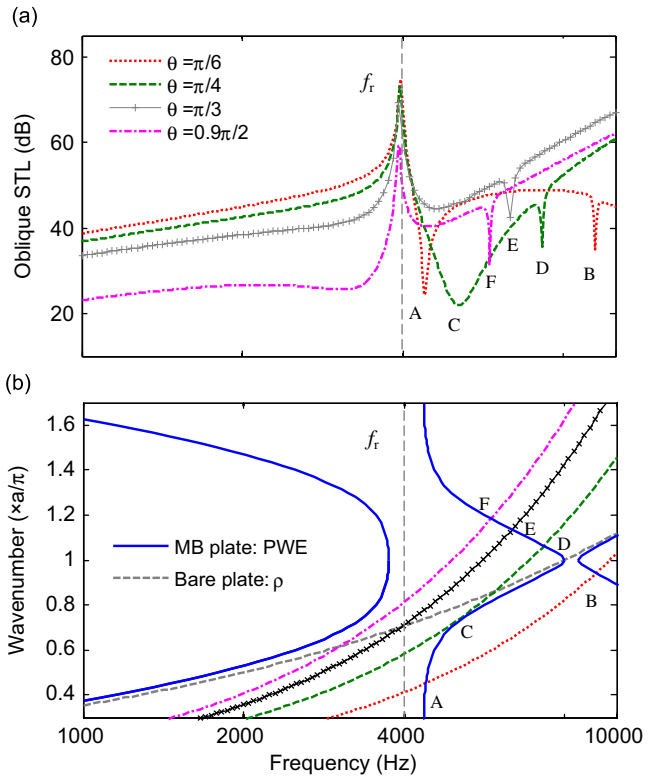

Fig. 7. (a) Evolution of the oblique STL of a metamaterial-based plate (f_r=4000 Hz) with changing incident angle θ. The azimuth angle is fixed to ϕ=0. (b) Wavenumber of the metamaterial-based (MB) plate and trace wavenumber of incident sound waves.

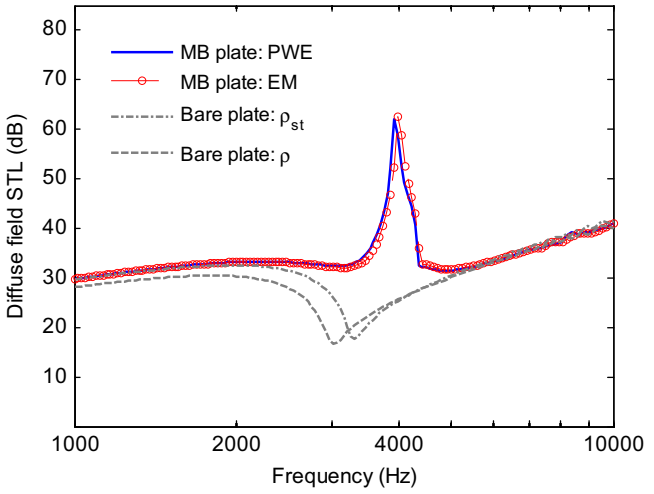

Fig. 8. The diffuse field STL of a metamaterial-based plate (f_r=4000 Hz) and two bare plates. The acronyms MB and EM refer to "metamaterial-based" and "effective medium", respectively.

4. Extremely thin plates

The aim of the above section is to increase the STL of a thin plate similar in thickness to existing plate structures in engineering. In contrast, in this section, we attempt to introduce an extremely thin plate into the construction of a metamaterial-based thin plate. This is motivated by the need for designing low-frequency sound insulation materials. We expect that, by using an extremely thin plate, the attached resonators can play a more important role, thus give rise to a higher STL around the resonance frequencies, as well as a broader bandwidth of frequencies with improved STL.

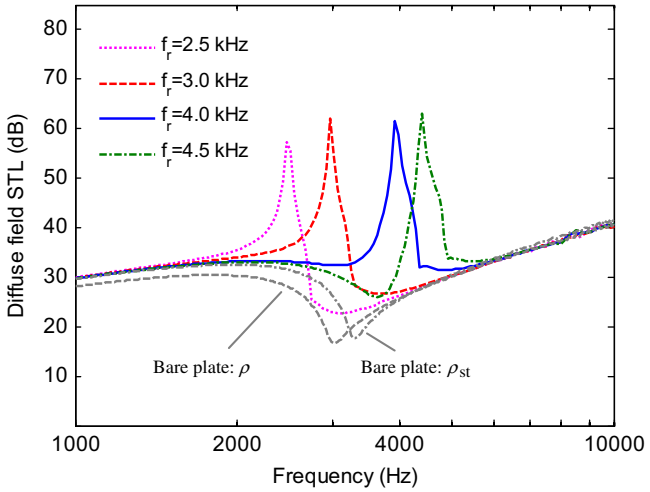

Fig. 9. Evolution of diffuse field STL of a metamaterial-based plate with changing resonator frequency f_r.

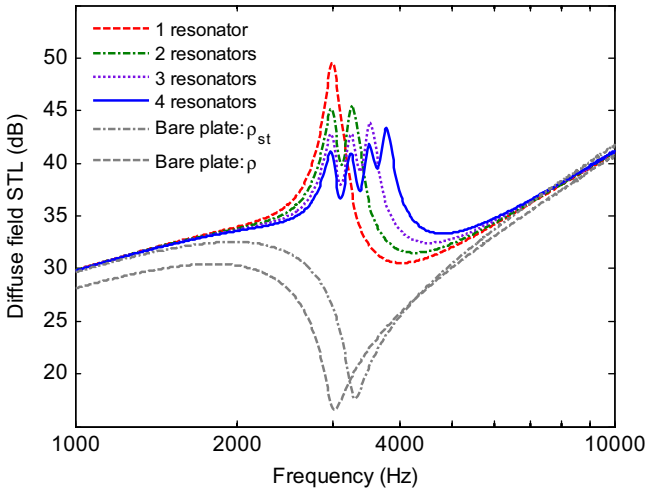

Fig. 10. Diffuse field STL of metamaterial-based plates with $N\,(=1, 2, 3, 4)$ attached resonators in each unit cell, $\eta_{r,j}=0.05$. The resonator parameters are chosen such that for $N=1$, $\gamma=m_r/\rho Sh=0.2$, and $f_r=3000$ Hz; for $N=2$, $\gamma_j=m_{r,j}/\rho Sh=0.2/2$ $(j=1,2)$, and $(f_{r,1}, f_{r,2})=(3000, 3250)$ Hz; for $N=3$, $\gamma_j=0.2/3$ $(j=1,2,3)$, and $(f_{r,1}, f_{r,2}, f_{r,3})=(3000, 3250, 3500)$ Hz; for $N=4$, $\gamma_j=0.2/4$ $(j=1, 2, 3, 4)$, and $(f_{r,1}, f_{r,2}, f_{r,3}, f_{r,4})=(3000, 3250, 3500, 3750)$ Hz.

Fig. 11 shows the diffuse field STL of a bare plate and that of four metamaterial-based plates with the same surface mass density. In each unit cell of the metamaterial-based plates, there are 12 attached resonators. They are designed with identical mass (i.e., $\gamma_j=m_{r,j}/\rho Sh=\gamma/12$) but slightly detuned resonance frequencies, being chosen such that: $f_{r,\,j}=100+(j-1)\times 100/11$ Hz, where $j=1, 2,\ldots, 12$. The comparisons in Fig. 11 indicate that, when the total surface mass density of a metamaterial-based plate is fixed, the thinner the plate is the higher the STL can be obtained at the resonance frequencies and the broader the improved bandwidth can be achieved. In addition, by using thinner plates, the mass ratio of the resonators γ becomes larger, thus the STL dip frequency [approximated by $f_r(1+\gamma)^{1/2}$, see Fig. 3 for reference] is shifted to some higher frequency range. Fig. 11 shows that, as compared with a bare plate with the same surface mass density, more than 5 dB average increase of STL can be achieved by a metamaterial-based thin plate (0.2 mm) over a low-frequency band (100–200 Hz).

5. Conclusions

In this paper, we have investigated sound transmission through metamaterial-based thin plates consisting of multiple subwavelength arrays of spring–mass resonators attached to an unbounded homogenous thin plate. Two analytical wave approaches were developed for the calculation of diffuse field sound transmission loss (STL) of metamaterial-based thin plates. One is based on the plane wave expansion (PWE) formulations that are suitable to deal with general periodic arrays of resonators. The other one is an effective medium method which can be performed with much less effort than the PWE

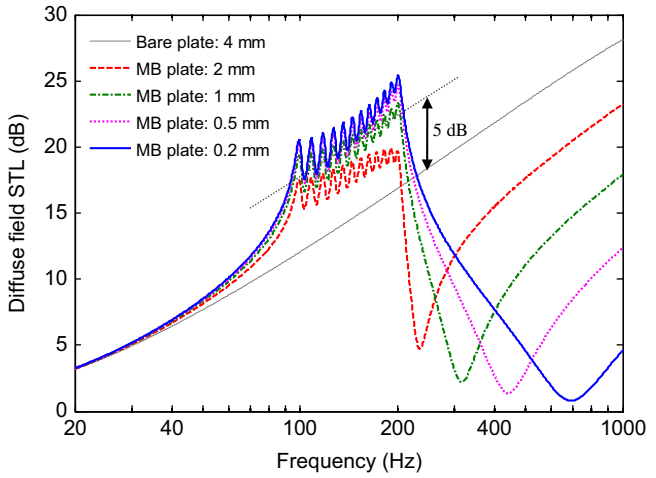

Fig. 11. Comparisons of the diffuse field STL of several plate systems with the same surface mass density. The metamaterial-based (MB) plates are designed with 12 slightly detuned resonators attached within each unit cell; the resonance frequency of the nth resonator is chosen following the formula: $f_{r,j}=100+(j-1)\times 100/11$, where $j=1, 2,\ldots, 12$. The resonator masses are chosen such that for $h=2$ mm, $\gamma=1$, $\gamma_j=m_{r,j}/\rho Sh=1/12$; for $h=1$ mm, $\gamma=3$, $\gamma_j=3/12$; for $h=0.5$ mm, $\gamma=7$, $\gamma_j=7/12$; for $h=0.2$ mm, $\gamma=19$, $\gamma_j=19/12$. The plate material properties are the same as in Table 1, and loss factor of the resonators is 0.05.

method but is only valid for the case of subwavelength resonator arrays, i.e., the case where the spacing between adjacent attached resonators is much smaller than the flexural wavelength of the host thin plate.

Numerical examples show that the STL of a metamaterial-based can deviate a lot from that of a bare plate with the same surface mass density. For the case of a single array of resonators, if the resonance frequency of the resonators is tuned to the mass-law region, the metamaterial-based plate can result in much higher diffuse field STL around the resonance frequency than that of a bare plate with the same surface mass density. However, a STL dip occurs at a frequency immediately above the resonance frequency. Such a behavior of a metamaterial-based plate is understood by the effective dynamic mass density. Further, if the resonance frequency is tuned to the coincidence region, the metamaterial-based plate can result in a significantly improved diffuse filed STL over the whole coincidence region; and outside this region it exhibits almost the same performance as that of a bare plate with identical surface mass. The frequency band of increased STL in a metamaterial-based plate can be broadened significantly by replacing a single resonator in each unit cell with multiple smaller appropriately damped resonators. It is also demonstrated that by using an extremely thin plate to construct a metamaterial-based plate, the construction may be utilized as a potential sound insulation material with good performance at low frequencies (<200 Hz).

Acknowledgments

This work was supported by the National Natural Science Foundation of China (Grant Nos. 51075392, 11004249 and 11004250). Part of this work was carried out when the first author was on study leave as a visiting student at ISVR, University of Southampton. The author gratefully acknowledges the hospitality of ISVR. Many thanks are due to Prof. B. R. Mace for his supervision of the first author at ISVR.

Appendix. Matrices and vectors in Eq. (26)

The plate stiffness matrix is

$$[\mathbf{K}_{\mathrm{p}}]=DS\begin{bmatrix}\left[\sum\limits_{s=x,y}(\mathbf{k}+\mathbf{G}_1)_s^2\right]^2 & 0 & \cdots & 0\\ 0 & \left[\sum\limits_{s=x,y}(\mathbf{k}+\mathbf{G}_2)_s^2\right]^2 & \cdots & \vdots\\ \vdots & \vdots & \ddots & 0\\ 0 & \cdots & 0 & \left[\sum\limits_{s=x,y}(\mathbf{k}+\mathbf{G}_{\overline{N}})_s^2\right]^2\end{bmatrix}. \tag{A1}$$

The fluid loading matrix is

$$[\mathbf{C}_\mathrm{f}] = 2\rho_0\omega S \begin{bmatrix} k_{z,\mathbf{G}_1}^{-1} & 0 & \cdots & 0 \\ 0 & k_{z,\mathbf{G}_2}^{-1} & \cdots & \vdots \\ \vdots & \vdots & \ddots & 0 \\ 0 & \cdots & 0 & k_{z,\mathbf{G}_{\overline{N}}}^{-1} \end{bmatrix}. \tag{A2}$$

The plate mass matrix is

$$[\mathbf{M}_\mathrm{p}] = \rho h S \begin{bmatrix} 1 & 0 & \cdots & 0 \\ 0 & 1 & \cdots & \vdots \\ \vdots & \vdots & \ddots & 0 \\ 0 & \cdots & 0 & 1 \end{bmatrix}_{\overline{N}\times\overline{N}}. \tag{A3}$$

The dynamic stiffness matrix of resonators is

$$[\mathbf{D}_\mathrm{r}] = \sum_{j=1}^{N} D_{\mathrm{r},j}[\mathbf{P}_j\mathbf{P}_j'], \tag{A4}$$

where

$$\mathbf{P}_j = \left[\mathrm{e}^{\mathrm{i}\mathbf{G}_1\cdot\mathbf{r}_j} \quad \mathrm{e}^{\mathrm{i}\mathbf{G}_2\cdot\mathbf{r}_j} \quad \cdots \quad \mathrm{e}^{\mathrm{i}\mathbf{G}_{\overline{N}}\cdot\mathbf{r}_j} \right]^\mathrm{T},$$

$$\mathbf{P}_j' = \left[\mathrm{e}^{-\mathrm{i}\mathbf{G}_1\cdot\mathbf{r}_j} \quad \mathrm{e}^{-\mathrm{i}\mathbf{G}_2\cdot\mathbf{r}_j} \quad \cdots \quad \mathrm{e}^{-\mathrm{i}\mathbf{G}_{\overline{N}}\cdot\mathbf{r}_j} \right].$$

The vector of plate displacement coefficients is

$$\{\mathbf{W}_\mathbf{G}\} = \left\{ W_{\mathbf{G}_1} \quad W_{\mathbf{G}_2} \quad \cdots \quad W_{\mathbf{G}_{\overline{N}}} \right\}^\mathrm{T}. \tag{A5}$$

The vector of excitation is

$$\left\{\boldsymbol{\delta}_{\mathbf{0}-\mathbf{G}}\right\} = \left\{ 0 \quad \cdots \quad 0 \quad 1 \quad 0 \quad \cdots \quad 0 \right\}_{\overline{N}\times 1}^\mathrm{T}. \tag{A6}$$

References

[1] D.R. Smith, W.J. Padilla, D.C. Vier, S.C. Nemat-Nasser, S. Schultz, Composite medium with simultaneously negative permeability and permittivity, *Physical Review Letters* 84 (2000) 4184.
[2] R.A. Shelby, D.R. Smith, S. Schultz, Experimental verification of a negative index of refraction, *Science* 292 (2001) 77–79.
[3] Z. Liu, X. Zhang, Y. Mao, Y.Y. Zhu, Z. Yang, C.T. Chan, P. Sheng, Locally resonant sonic materials, *Science* 289 (2000) 1734–1736.
[4] J. Li, C.T. Chan, Double-negative acoustic metamaterial, *Physical Review E* 70 (2004) 055602(R).
[5] N. Fang, D. Xi, J. Xu, M. Ambati, W. Strituravanich, C. Sun, X. Zhang, Ultrasonic metamaterials with negative modulus, *Nature Materials* 5 (2006) 452–456.
[6] P. Sheng, J. Mei, Z. Liu, W. Wen, Dynamic mass density and acoustic metamaterials, *Physica B* 394 (2007) 256–261.
[7] G.W. Milton, J.R. Willis, On modifications of Newton's second law and linear continuum elastodynamics, *Proceedings of the Royal Society A* 463 (2007) 855–880.
[8] K.M. Ho, Z. Yang, X.X. Zhang, P. Sheng, Measurements of sound transmission through panels of locally resonant materials between impedance tubes, *Applied Acoustics* 66 (2005) 751–765.
[9] E.P. Calius, X. Bremaud, B. Smith, A. Hall, Negative mass sound shielding structures: early results, *Physica Status Solidi B* 246 (2009) 2089–2097.
[10] G. Wang, X. Wen, J. Wen, Y. Liu, Quasi-one-dimensional periodic structure with locally resonant band gap, *Journal of Applied Mechanics* 73 (2006) 167–170.
[11] Y. Xiao, J. Wen, X. Wen, Longitudinal wave band gaps in metamaterial-based elastic rods containing multi-degree-of-freedom resonators, *New Journal of Physics* 14 (2012) 033042.
[12] D. Yu, Y. Liu, G. Wang, H. Zhao, J. Qiu, Flexural vibration band gaps in Timoshenko beams with locally resonant structures, *Journal of Applied Physics* 100 (2006) 124901.
[13] Y. Xiao, J. Wen, X. Wen, Broadband locally resonant beams containing multiple periodic arrays of attached resonators, *Physics Letters A* 376 (2012) 1384–1390.
[14] G. Wang, Band Gap Formation Mechanisms and Vibration Attenuation Characteristics of Locally Resonant Phononic Crystals, PhD Thesis, National University of Defense Technology, 2005.
[15] X. Wen, J. Wen, D. Yu, G. Wang, Y. Liu, X. Han, *Phononic Crystals (in Chinese)*, National Defense Industry Press, Beijing, 2009.
[16] M. Oudich, Y. Li, B.M. Assouar, Z. Hou, A sonic band gap based on the locally resonant phononic plates with stubs, *New Journal of Physics* 12 (2010) 083049.
[17] J.C. Hsu, Local resonances-induced low-frequency band gaps in two-dimensional phononic crystal slabs with periodic stepped resonators, *Journal of Physics D: Applied Physics* 44 (2011) 055401.
[18] Y. Xiao, J. Wen, X. Wen, Flexural wave band gaps in locally resonant thin plates with periodically attached spring–mass resonators, *Journal of Physics D: Applied Physics* 45 (2012) 195401.
[19] Z. Yang, J. Mei, M. Yang, N.H. Chan, P. Sheng, Membrane-type acoustic metamaterial with negative dynamic mass, *Physical Review Letters* 101 (2008) 204301.
[20] Z. Yang, H.M. Dai, N.H. Chan, G.C. Ma, P. Sheng, Acoustic metamaterial panels for sound attenuation in the 50–1000 Hz regime, *Applied Physics Letters* 96 (2010) 041906.

[21] C.J. Naify, C.M. Chang, G. McKnight, S. Nutt, Transmission loss and dynamic response of membrane-type locally resonant acoustic metamaterials, *Journal of Applied Physics* 108 (2010) 114905.
[22] Y. Zhang, J. Wen, Y. Xiao, X. Wen, J. Wang, Theoretical investigation of the sound attenuation of membrane-type acoustic metamaterials, *Physics Letters A* 376 (2012) 1489–1494.
[23] J.P. Den Hartog, *Mechanical Vibrations*, 4th ed. McGraw-Hill, New York, 1956.
[24] J.Q. Sun, M.R. Jolly, M.A. Norris, Passive, adaptive and active tuned vibration absorbers – a survey, *Journal of Vibration and Acoustics* 117 (1995) 234–242.
[25] M. Strasberg, D. Feit, Vibration damping of large structures induced by attached small resonant structures, *Journal of the Acoustical Society of America* 99 (1996) 335–344.
[26] M.J. Brennan, Characteristics of a wideband vibration neutralizer, *Noise Control Engineering Journal* 45 (1997) 201–207.
[27] G. Maidanik, Induced damping by a nearly continuous distribution of nearly undamped oscillators: linear analysis, *Journal of Sound and Vibration* 240 (2001) 717–731.
[28] D.J. Thompson, A continuous damped vibration absorber to reduce broad-band wave propagation in beams, *Journal of Sound and Vibration* 311 (2008) 824–842.
[29] M.R. Jolly, J.Q. Sun, Passive tuned vibration absorbers for sound radiation reduction from vibrating panels, *Journal of Sound and Vibration* 191 (1996) 577–583.
[30] C.R. Fuller, J.P. Maillard, M. Mercadal, A.H. von Flotow, Control of aircraft interior noise using globally detuned vibration absorbers, *Journal of Sound and Vibration* 203 (1997) 745–761.
[31] Y.M. Huang, C.R. Fuller, The effects of dynamic absorbers on the forced vibration of a cylindrical shell and its coupled interior sound field, *Journal of Sound and Vibration* 200 (1997) 401–418.
[32] S.J. Esteve, M.E. Johnson, Reduction of sound transmission into a circular cylindrical shell using distributed vibration absorbers and Helmholtz resonators, *Journal of the Acoustical Society of America* 112 (2002) 2840–2848.
[33] M.R.F. Kidner, C.R. Fuller, B. Gardner, Increase in transmission loss of single panels by addition of mass inclusions to a poro-elastic layer: experimental investigation, *Journal of Sound and Vibration* 294 (2006) 466–472.
[34] K. Idrisi, M.E. Johnson, A. Toso, J.P. Carneal, Increase in transmission loss of a double panel system by addition of mass inclusions to a poro-elastic layer: a comparison between theory and experiment, *Journal of Sound and Vibration* 323 (2009) 51–66.
[35] C.Q. Howard, Transmission loss of a panel with an array of tuned vibration absorbers, *Acoustics Australia* 36 (2008) 98–103.
[36] M.M. Sigalas, E.N. Economou, Elastic waves in plates with periodically placed inclusions, *Journal of Applied Physics* 75 (1994) 2845–2850.
[37] J.C. Hsu, T.T. Wu, Efficient formulation for band-structure calculations of two-dimensional phononic-crystal plates, *Physical Review B* 74 (2006) 144303.
[38] D.J. Mead, K.K. Pujara, Space-harmonic analysis of periodically supported beams: response to convected random loading, *Journal of Sound and Vibration* 14 (1971) 525–541.
[39] B.R. Mace, Periodically stiffened fluid-loaded plates, I: response to convected harmonic pressure and free wave propagation, *Journal of Sound and Vibration* 73 (1980) 473–486.
[40] B.R. Mace, The vibration of plates on two-dimensionally periodic point supports, *Journal of Sound and Vibration* 192 (1996) 629–643.
[41] J. Legault, N. Atalla, Numerical and experimental investigation of the effect of structural links on the sound transmission of a lightweight double panel structure, *Journal of Sound and Vibration* 324 (2009) 712–732.
[42] J. Legault, A. Mejdi, N. Atalla, Vibro-acoustic response of orthogonally stiffened panels: the effects of finite dimensions, *Journal of Sound and Vibration* 330 (2011) 5928–5948.
[43] F.X. Xin, T.J. Lu, Analytical modeling of fluid loaded orthogonally rib-stiffened sandwich structures: sound transmission, *Journal of the Mechanics and Physics of Solids* 58 (2010) 1374–1396.
[44] Y. Wu, Y. Lai, Z. Zhang, Effective medium theory for elastic metamaterials in two dimensions, *Physical Review B* 76 (2007) 205313.
[45] M.R.F. Kidner, K. Idrisi, J.P. Carneal, M.E. Johnson, Comparison of experiment, finite element and wave based models for mass inclusions in poro-elastic layers, *Proceedings of 14th International Congress on Sound and Vibration*, *Carins*, *Australia*, 2007, Paper 577.
[46] K. Idrisi, M.E. Johnson, D. Theurich, J.P. Carneal, A study on the characteristic behavior of mass inclusions added to a poro-elastic layer, *Journal of Sound and Vibration* 329 (2010) 4136–4148.
[47] L. Brillouin, *Wave Propogation in Periodic Structures*, Dover, New York, 1946.
[48] F. Fahy, P. Gardonio, *Sound and Structural Vibration: Radiation, Transmission and Response*, 2nd ed. Academic Press, Oxford, 2007.
[49] C. Hopkins, *Sound Insulation: Theory into Practice*, Butterworth-Heinemann, Oxford, 2007.
[50] Y. Xiao, B.R. Mace, J. Wen, X. Wen, Formation and coupling of band gaps in a locally resonant elastic system comprising a string with attached resonators, *Physics Letters A* 375 (2011) 1485–1491.
[51] D.J. Mead, Free wave propagation in periodically supported, infinite beams, *Journal of Sound and Vibration* 11 (1970) 181–197.